Defect states in doped and compensated *a*-Si:H

R. A. Street, D. K. Biegelsen, and J. C. Knights
Xerox Palo Alto Research Center, Palo Alto, California 94304
(Received 24 November 1980)

Luminescence, electron spin resonance (ESR), optical absorption, conductivity, and composition data are measured on doped and compensated hydrogenated amorphous silicon. In material singly doped with boron or phosphorus, a variety of experiments indicates the introduction of a large defect density (up to 10^{18} cm^{-3}) of the dangling-bond type. Compensation increases the luminescence efficiency, but the luminescence peak shifts strongly to lower energy. Compensation reduces the ESR resonance at $g = 2.0055$, but a broad resonance characteristic of a hole trap remains. We deduce that compensation reduces the dangling-bond density, but introduces a new band of localized states above the valence-band edge. We associate these new states with boron-phosphorus complexes whose origin is a chemical interaction occurring during deposition. Changes in the dangling-bond density with doping and compensation lead us to propose an autocompensation mechanism of defect formation. Also reported is the first observation of a metastable light-induced ESR signal in *a*-Si:H.

I. INTRODUCTION

The photoluminescence of undoped *a*-Si:H is now comparatively well understood.[1-3] The dominant transition is between states near the band edges giving a broad luminescence peak at ~1.4 eV, and having a moderate Stokes shift.[4] The intensity of the luminescence is controlled predominately by dangling-bond defects as observed in electron spin resonance (ESR).[2] When these are present in concentrations less than ~10^{17} cm^{-3}, the luminescence efficiency at 10 K approaches unity. At elevated temperatures the luminescence is quenched by a mechanism involving the separation of carrier pairs followed by capture at dangling bonds.[5,6] The importance of defect states in the gap for nonradiative recombination is common in semiconductors, and much effort has gone into making low defect density *a*-Si:H.

Electron spin resonance (ESR) in *a*-Si:H is also fairly well understood.[7,8] The single, featureless, and slightly asymmetric line at $g = 2.0055$ arises from strongly localized neutral silicon dangling bonds randomly oriented relative to the external magnetic field. The energy level associated with the neutral state of this defect lies below the center of the band gap whereas the negative state (doubly occupied and diamagnetic) lies above midgap. The spin density in undoped material, for which the Fermi energy is near midgap, thus equals the density of dangling bonds which can vary from $\leq 10^{20}$ cm^{-3} down to below the level of detectability ($<10^{15}$ cm^{-3}) depending on deposition conditions.[2] In *a*-Si:H samples deposited under conditions such that an observable spin signal exists in *undoped* material, it is known that when doped either *p* or *n* type (but keeping the deposition conditions otherwise the same) the dangling-bond signal disappears as the Fermi level is moved towards the band edges.[9] The decreasing ESR signal does not indicate a reduced defect density, but rather a decreasing fraction of singly occupied defects due to the shift of E_F past the appropriate energy level.[10] As might be expected, for deposition conditions producing a low density of gap states in undoped material, less doping is needed to quench the defect ESR than for conditions producing high gap state densities.

Light-induced electron spin resonance (LESR) has also been useful in elucidating the gap states.[10,11] Like luminescence, LESR is a nonequilibrium process. It reveals states which are paramagnetic before recombination of the excited carriers occurs. In undoped material a relatively weak pair of lines is observed. From the correlation with luminescence the broad ($\Delta H_{pp} \sim 18$ G) line at $g \sim 2.013$ has been assigned to band-tail holes and a narrow ($\Delta H_{pp} \sim 5$ G) line at $G \sim 2.004$ has been assigned to band-tail electrons.[10] The same line shapes are also observed by equilibrium ESR in heavily doped *a*-Si:H (Refs. 7 and 9 and see Sec. III) which gives additional evidence for these assignments. The existence of these lines in undoped material demonstrates that the states are intrinsic to the silicon and not specifically associated with any dopant.

One result of a low defect density is that electronic doping of *a*-Si:H is possible.[12,13] A doping level of typically $10^{-4}[PH_3]$ in SiH_4 is required to shift the Fermi energy up to the band tails.[13] This corresponds to a doping concentration of about 5×10^{18} cm^{-3} which is well in excess of what is required given the estimated density of states in the gap that have to be compensated by the doping.[14] One reason for the excess dopant required is that most of the impurity atoms may bond in nondoping configurations (threefold-coordinated phosphorus for example). In the case of As doping there is

direct evidence that only about 10% of the As atoms are fourfold coordinated and electronically active.[15] However, an additional reason is that the doping process might introduce defects into the material which therefore requires extra doping to move the Fermi energy. There is already some evidence that this is indeed the case. The luminescence efficiency of doped samples decreases as the doping level increases,[16,17] and the luminescence decay is characteristic of material with defects.[18] Another indication is the poor performance of doped material for photovoltaic devices. Part of the purpose of this paper is to provide more detailed evidence of defect introduction by doping and to suggest reasons why this occurs. It is argued that studies of compensated samples can separate the various models and new data on material doped with different amounts of both boron and phosphorus are presented.

There have been several studies of luminescence in doped a-Si:H all of which agree on the basic result that luminescence is quenched by doping both p and n type.[16-18] At doping levels of about 10^{-3}, a peak near 0.9 eV is observed in the luminescence spectrum[16,17] which has been attributed to a transition through defect levels, specifically dangling bonds.[19] The only report of luminescence from compensated a-Si:H finds a peak at ~1.0 eV for nominal doping levels of $\sim 1.7 \times 10^{-3}$ and associates this with the defect transition.[17] In this paper we report measurements on both doped and compensated samples with doping levels in the range 0–10^{-2}. Measurements are made of the luminescence spectra, intensity, temperature dependence, and time decay, as well as ESR and light-induced ESR, optical absorption, conductivity, and compositional analysis.

II. SAMPLE PREPARATION AND CHARACTERIZATION

The samples were prepared by plasma deposition as described elsewhere.[2] The deposition conditions used were those known to give undoped a-Si:H with very low defect density: substrate temperature 230 °C, low rf power (2 W), and SiH_4 with no carrier gas. The dopant gasses were PH_3 and B_2H_6 prediluted in SiH_4.

The dopant concentration of some samples was measured by secondary-ion mass spectroscopy (SIMS), and the results are given in Table I. The measurements were made using an O^- beam to avoid charging effects, since the samples are deposited on glass substrates. This reduced the sensitivity because the sputtering rate is low. Concentration profiles were measured in a few cases and variations with depth of typically 20–30% were found. This value is therefore taken as the estimated uncertainty. For both boron and phosphorus single doping the concentration is above the molecular fraction of dopant gas in SiH_4 by a factor 3 to 5. Similar enhancement factors for boron have been reported previously by Zesch *et al.*[20] The results for compensated samples are very interesting. When the boron and phosphorus doping is at roughly equal levels, the enhancement is close to that found for single doping. However, when the doping levels are very different, the minority species tends to be incorporated in the film much more efficiently. The most striking example is with the $10^{-3}[PH_3]$, $10^{-4}[B_2H_6]$ sample in which the enhancement factor for boron is 23 compared to about 4 for the 10^{-3} compensated sample. A similar increase of phosphorus is found when PH_3 is the minority dopant. Evidently the deposition process has a tendency to equalize the two dopant concentrations in the films. It is therefore clear that there is some cooperative reaction during the deposition and the formation of a boron-phosphorus pair, or some similar complex, either as a gas-phase or surface reaction, is strongly indicated. As we shall see, this cooperative process is evident in the luminescence data. In all the data reported below the dopant levels are stated as the molecular fraction of PH_3 or B_2H_6 in SiH_4 in the reactor gas. We refer to this as the nominal doping level. The true concentrations in the material can be estimated from the enhancement factors given in Table I.

TABLE I. Result of SIMS measurements of ^{11}B and ^{31}P concentrations. The enhancement factors E_P and E_B are the ratios of the measured to the nominal concentrations.

Nominal concentrations P	Nominal concentrations B	Enhancement E_P	Enhancement E_B
10^{-3}		5.2	
10^{-3}	10^{-4}	4.3	23
10^{-3}	10^{-3}	3.5	4.2
10^{-3}	4×10^{-3}	9.4	4.1
	10^{-3}		3
3×10^{-4}	10^{-3}	9.3	7.1
3×10^{-3}	10^{-3}	4.8	13.3
10^{-4}	10^{-4}	8	4.5
3×10^{-4}	3×10^{-4}	5.8	6.2

Figure 1 shows the deposition rate for a variety of doped and compensated samples. In agreement with other reports[21] we find that boron doping substantially enhances the deposition rate such that at a nominal doping level of $4\times10^{-3}[B_2H_6]$ the increase is about 40%. On the other hand, phosphorus doping seems to reduce the deposition rate. This can be seen in Fig. 1 for two compensated

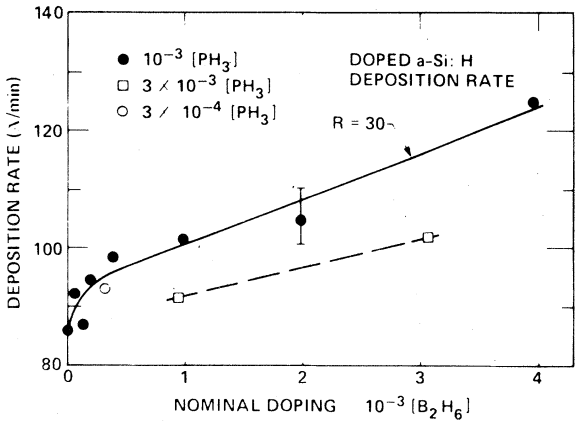

FIG. 1. Deposition rate for doped and compensated *a*-Si:H samples. The deposition time is approximately 2 h for each sample. *R* is the slope of the linear region expressed as the fractional increase in the deposition rate divided by the estimated true boron concentration obtained using the correction factors from Table I.

samples and by comparing with undoped samples which have a deposition rate of ~100 Å/min. It is therefore clear that the dopant gases have an influence on the deposition process which far exceeds their relative concentration in the plasma. In addition the deposition rate increases particularly rapidly with the addition of small quantities of B_2H_6 to $10^{-3}[PH_3]$ material. We associate this effect to the large enhancement of the minority dopant concentration discussed above.

Measurements of the infrared spectrum of a 10^{-3} compensated sample showed no discernible change in the hydrogen bonding compared to an equivalent undoped sample.[22] The Si-H stretching modes were predominately at 2000 cm^{-1}. Furthermore, the fracture surface of a compensated sample shows no sign of columnar growth.[23] We therefore conclude that doping and compensation do not substantially change the sample microstructure or hydrogen bonding.

To demonstrate that electrical compensation is occurring, measurements of dc conductivity and the sign of the thermopower were made. The temperature dependence of dc conductivity of some samples is shown in Fig. 2. For a series of samples with $10^{-3}[PH_3]$ and variable concentrations of B_2H_6, electrical compensation occurs within a factor of 2 of the nominal compensation level of $10^{-3}[B_2H_6]$ in agreement with other data.[24] This particular composition was too resistive to determine the sign of the thermopower or to give reliable conductivity because of contact effects. However, all samples with more boron had positive thermopower, and all with less boron were negative. As seen in Fig. 2 the conductivity increases and the activation energy decreases as

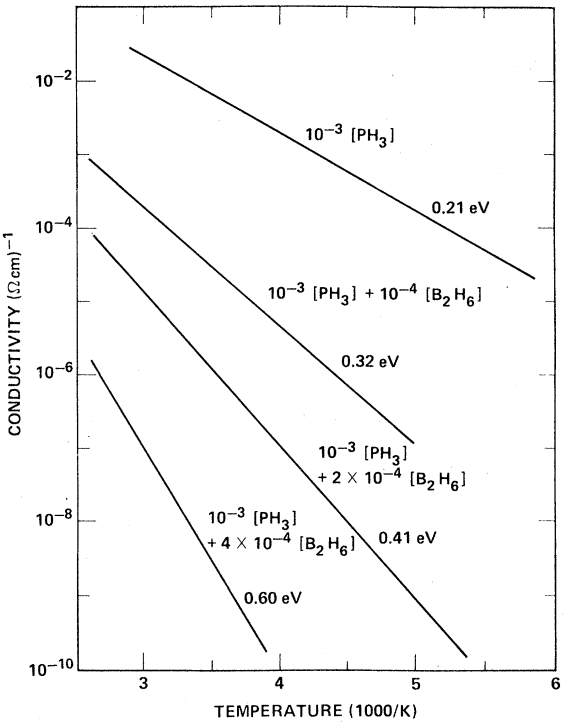

FIG. 2. dc conductivity versus inverse temperature for various doped and compensated *n*-type samples. The activation energies are indicated.

the boron concentration is reduced from the compensation value. The activation energy of 0.4 eV found for $10^{-3}[PH_3]$ and $2 \times 10^{-4}[B_2H_6]$ is roughly the same as that observed for $10^{-5}[PH_3]$. Even taking into account the different dopant incorporation rates, this indicates that in the compensated samples a much larger change in doping is required to move the Fermi energy than in lightly doped material.

III. RESULTS

A. Luminescence

1. Singly doped samples

The luminescence peak position and intensity of phosphorus- and boron-doped samples is shown in Fig. 3 as a function of the nominal doping level. The results are almost identical for the two dopants. Both quench the luminescence, particularly at doping levels above 10^{-4}, and the luminescence becomes undetectable above 10^{-2}. At high doping levels the defect luminescence near 0.9 eV (Ref. 19) is the dominant emission. There is a small range of doping at which both the 0.9-eV band and the band-edge transition are observed and an example of this is shown in Fig. 6. The emergence of the defect band is seen clearly by the abrupt

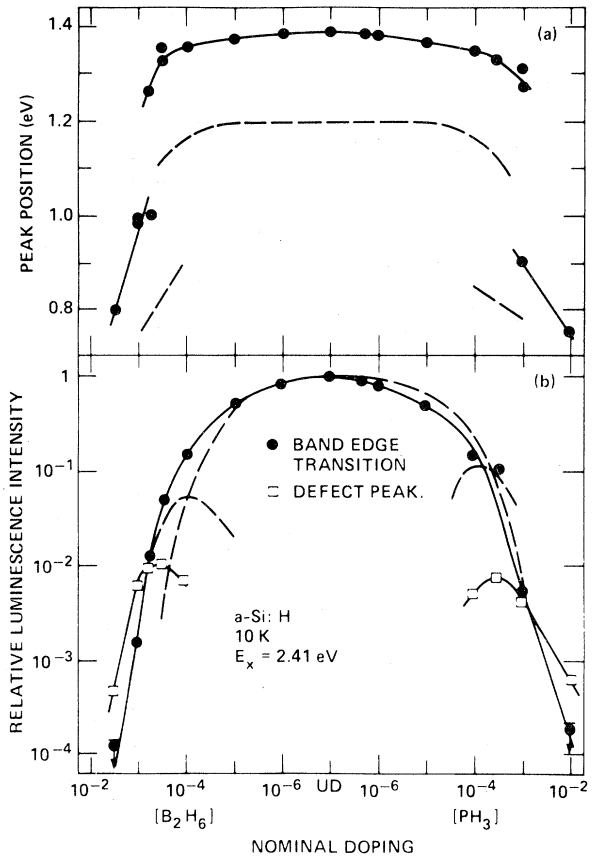

FIG. 3. (a) peak position and (b) intensity of the luminescence of doped samples. The dashed curves are equivalent data reported by Fischer *et al.* (Ref. 16) at a measurement temperature of 77 K.

decrease in the peak position by about 0.4 eV seen in Fig. 3. Another feature evident from Fig. 3 is that the peak energy of either band is not constant, but decreases at doping levels above 10^{-3}. The decrease is more pronounced with boron doping than with phosphorus.

These observations are in qualitative agreement with those reported by other groups. In particular, similar data of Fischer *et al.*[16] are shown in Fig. 3 for comparison. Although the trends are clearly the same, there are notable quantitative differences. One is that the defect luminescence is relatively more intense by about an order of magnitude. Secondly the defect luminescence dominates at doping levels which are an order of magnitude lower than ours and finally the peak energies are lower, particularly those of the band-edge transition. Part of this shift may be due to the higher measurement temperature (77 K). However, neither of the other differences can be explained in this way. (In our samples the ratio of the band edge to defect peak intensities does not change by more than 25% on raising the temperature to 80 K.) Instead we attribute them to the different deposition conditions for these samples and note that our earlier data[17] using material deposited from 5 mol% SiH_4–95 mol% Ar also differed from the present data quantitatively but not qualitatively. At present we cannot determine whether the effects are due to different dopant concentrations in the films, different doping efficiences or to some other mechanism. However, the comparison serves to indicate the magnitude of the variations that can be expected from samples prepared in different laboratories.

Our previous measurements of luminescence decay in doped samples indicated that the quenching of the band-edge transition was due to a high defect density in the doped samples.[17] We have also performed two other luminescence experiments that lead to the same conclusion. The first is the intensity dependence of the luminescence quantum efficiency at an elevated temperature, specifically 170 K. In undoped samples the quantum efficiency increases with intensity by an amount inversely dependent on the defect density.[6] The reason is a bimolecular luminescence process which competes with nonradiative recombination through defects. Figure 4 shows the results of this experiment for two lightly phosphorous-doped samples in which the enhancement observed is substantially less than in undoped samples. The quantum efficiency $y(G)$ is expected to vary with excitation intensity,

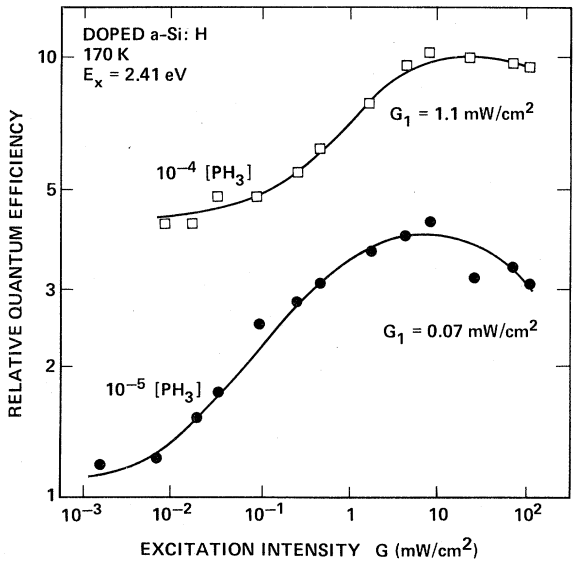

FIG. 4. The excitation-intensity dependence of luminescence for two phosphorus-doped samples. G_1 is the intensity at which the quantum efficiency y is doubled, based on a fit to Eq. (1), and is a measure of the defect density as described in Ref. 6.

G as

$$y(G) = y_0(1 + \gamma G/\beta^2 N_s^2), \quad (1)$$

where N_s is the defect density, y_0 is the quantum efficiency at the limit of low G, and γ and β are constants.[6] The data of Fig. 4 are fitted to this expression over the low-intensity region and the value of G_1 obtained is the excitation intensity for which

$$\gamma G_1 = \beta^2 N_s^2. \quad (2)$$

Comparison with undoped samples indicates a defect density of $\sim 1.5 \times 10^{16}$ cm^{-3} for $10^{-5}[PH_3]$ and $\sim 10^{17}$ cm^{-3} for $10^{-4}[PH_3]$ compared with $\sim 3 \times 10^{15}$ cm^{-3} in the undoped material prepared under the same deposition conditions.

The second experiment is the temperature dependence of the luminescence intensity which is shown in Fig. 5. At this point we are interested in the comparison of the undoped sample and the sample doped $10^{-4}[PH_3]$ and $10^{-3}[PH_3]$. Although the doping reduces the low-temperature efficiency by one or two orders of magnitude, the sets of data converge at about 200 K. Similar behavior is found in undoped material with differing defect densities.[6] This effect is interpreted as a transfer of the dominant nonradiative mechanism from tunnelling to defects at low temperature, to thermal ionization at high temperature.[6] The equivalent results of the doped samples strongly suggest that the low efficiency is due to an increase in the defect density and that the nonradiative mechanism is essentially the same as in undoped samples. From this conclusion we can estimate the defect density in the doped samples from the known relation between the luminescence intensity and the spin density in undoped material. In this way we obtain a defect density $\sim 3 \times 10^{17}$ cm^{-3} at a doping level of about 10^{-4} in rough agreement with the results of Fig. 4. Further evidence for a high defect density in doped material is obtained from light-induced ESR measurements as described in Sec. III B.

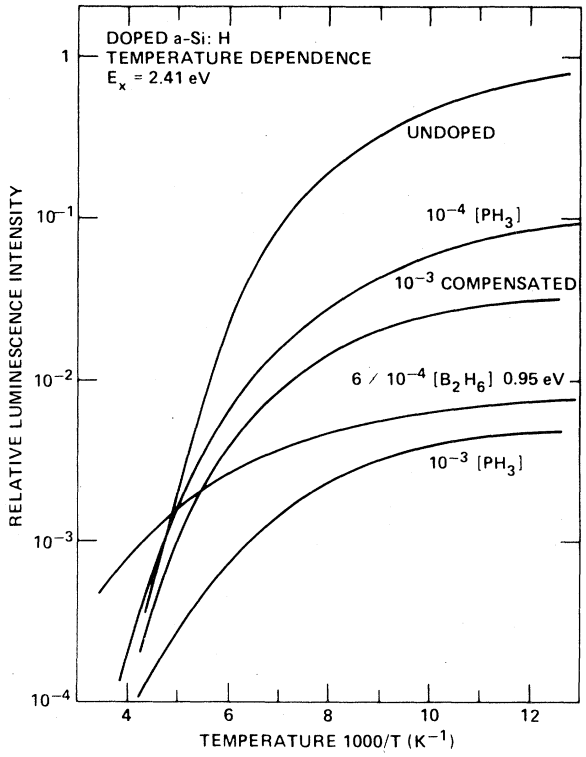

FIG. 5. Temperature dependence of luminescence intensity of various samples. The data are not corrected for the shift of the luminescence peak with temperature. Note that the intensities converge at high temperature except that of the defect luminescence.

2. *Compensated samples*

One reason for studying compensated samples is that they allow one to vary the doping and the position of the Fermi level independently. Based on the conclusion that doping introduces defects, it is important to know whether the defects are a consequence of the Fermi-energy position or solely of the chemistry of the deposition process. Our results concentrate on fairly heavy doping levels (above 10^{-4}) because these samples show the largest effects. Figure 6 shows examples of luminescence spectra of samples doped $10^{-3}[PH_3]$ and compensated with various amounts of boron. Figure 7 shows the peak position, intensity, and linewidth for the complete set of samples in this series, and Fig. 8 shows equivalent data for samples with $10^{-3}[B_2H_6]$ and variable phosphorus compensation. In both series compensation tends to increase the luminescence efficiency. For constant phosphorus (Fig. 7) the maximum luminescence occurs for $2 \times 10^{-4}[B_2H_6]$ and the efficiency increases by about an order of magnitude. In the other series the peak is at the nominal compensation level, and the increase is less, about a factor of 3.

At the nominal compensation the luminescence spectrum peaks at 1.02 eV in agreement with measurements by Austin *et al.*[17] Inspection of Fig. 3 shows that the defect luminescence line is at about this energy in $10^{-3}[B_2H_6]$ material although it is at 0.9 eV in the equivalent phosphorus-doped material. (Note that we do not consider these differences in energy of the defect peak to be significant because of the steady variation of energy with doping level shown in Fig. 3.) Thus a plausible interpretation is that the defect line is dominating in a compensated material as was deduced by Austin *et al.*[17] However, this turns out to be an incorrect

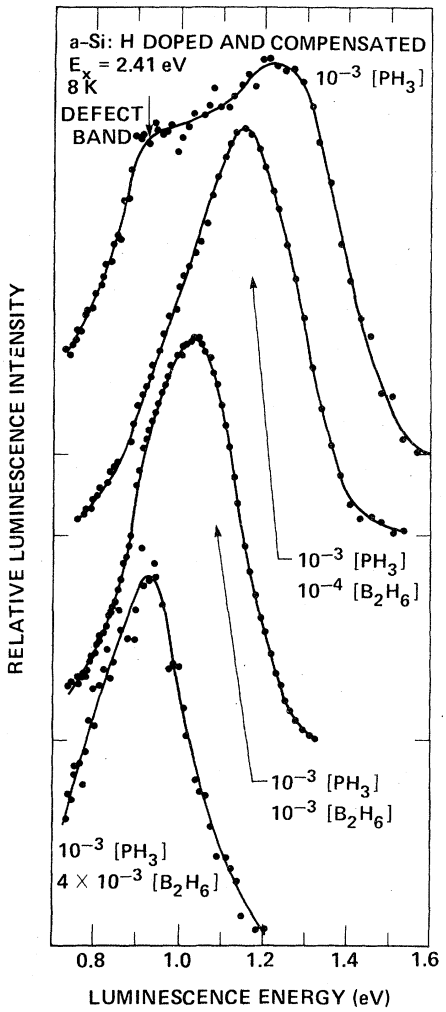

FIG. 6. Examples of luminescence spectra of doped and compensated samples. The spectra are normalized to the same peak height. The true relative intensities are given in Fig. 7.

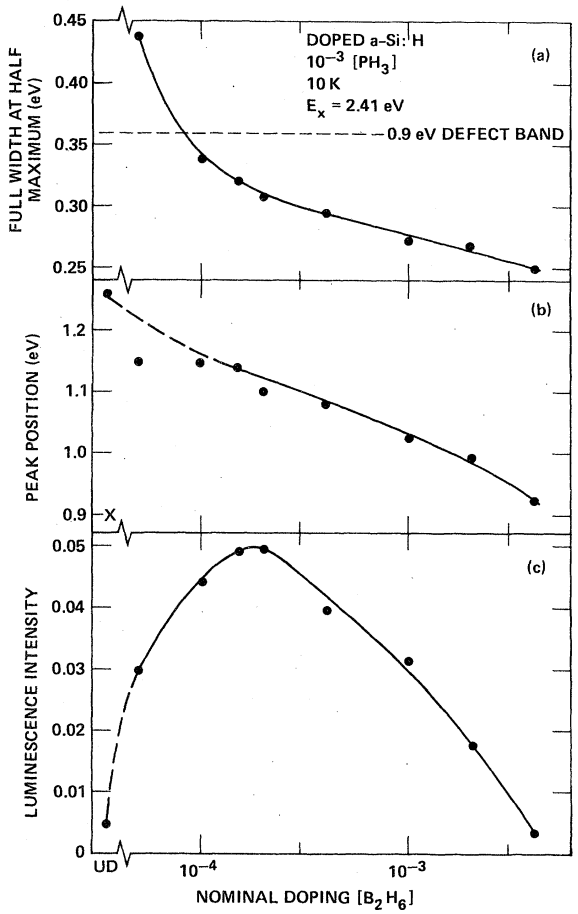

FIG. 7. Luminescence parameters of a compensation series with constant phosphorus (10^{-3}[PH_3]) and variable boron concentrations: (a) spectral width, (b) peak position, and (c) luminescence intensity normalized to the intensity (=unity) of undoped samples. Note the logarithmic doping scale.

deduction as is shown from the various observations described below.

In Fig. 7 it is seen that peak energy of the compensated samples varies with the compensation level. Reducing the boron content increases the peak energy steadily, and the extrapolated value corresponds to the band-edge transition, rather than the defect line. These trends are evident in the spectra of Fig. 6. Furthermore the linewidth of the spectrum decreases rapidly with compensation by boron (Fig. 7) to a value of 0.25 eV. This is much less than the known width of the defect band (~0.35 eV) (Ref. 19) but similar to that of the band edge transition in undoped samples. The spectra of the lightly compensated samples are also asymmetric (see Fig. 6) which we interpret as indicating the remanent of the defect line whose relative intensity is decreasing rapidly with compensation. Our conclusion is that the peak in the compensated sample is derived from the band-edge transition with a continuous evolution of this peak down in energy as the boron concentration increases.

The same conclusion holds for the series with constant boron and variable phosphorus, shown in Fig. 8. In this series the luminescence peak does not shift up in energy so much, but there is a distinct discontinuity between the 10^{-3}[B_2H_6] sample and the 10^{-3}[B_2H_6], 10^{-4}[PH_3] material. The small shift is probably because the band-edge peak is already unresolved from the defect line in the 10^{-3}[B_2H_6] sample. However, the change in the character of the band is more noticeable in the linewidth which decreases rapidly with compensation, again reaching a value of 0.25 eV. As be-

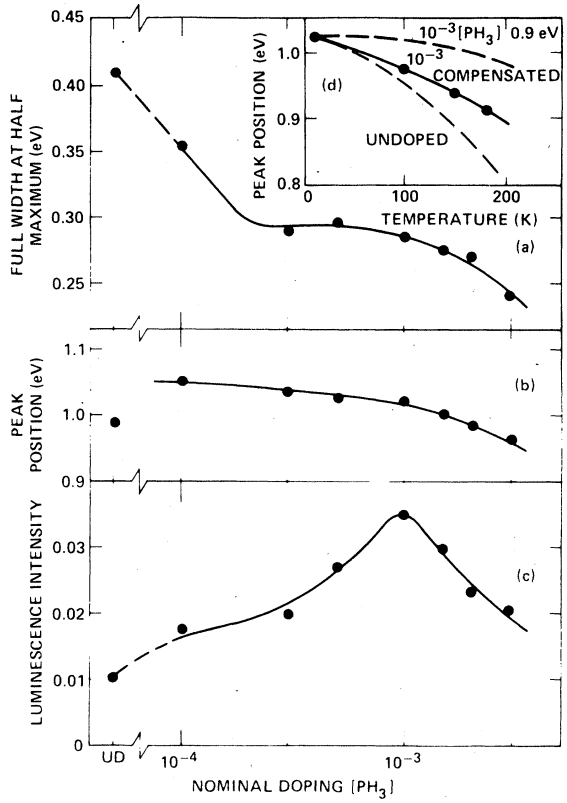

FIG. 8. Luminescence parameters of a compensation series with constant boron ($10^{-3}[B_2H_6]$) and variable phosphorus concentrations: (a) spectral width; (b) peak position; (c) luminescence intensity normalized to the intensity (=unity) of undoped sampled; and (d) temperature dependence of the peak energy for the nominally compensated samples compared to the undoped band-edge transiton and the 0.9-eV defect peak.

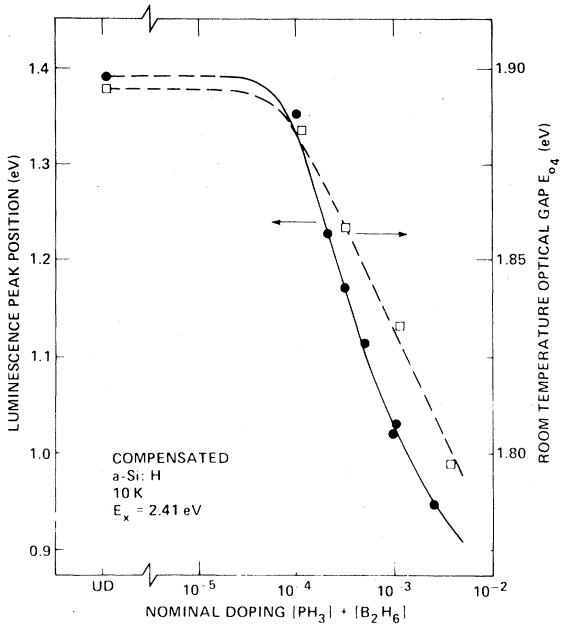

FIG. 9. Luminescence peak position for nominally compensated samples of differing doping level (left-hand scale). Also shown in the optical gap E_{04} defined as the energy at which $\alpha = 10^4$ cm^{-1} for the same samples (right-hand scale). Note that the luminescence peak shift is about five times larger than that of E_{04}.

fore, we attribute the decrease to the disappearance of the defect transition.

There are various other pieces of experimental evidence that the luminescence in the compensated material has a different character from the 0.9-eV defect peak and evolves continuously from the band-edge transition. Figure 5 shows temperature-dependence data. The thermal quenching of the compensated sample converges with that of undoped *a*-Si:H above 200 K, indicating that the mechanism of thermally activated ionization of electrons is essentially unchanged.[6] On the other hand the quenching of the 0.9-eV defect line occurs at a higher temperature and has been associated with an electron trapped at a deeper state.[19]

The inset in Fig. 8 shows the temperature dependence of the luminescence peak energy for the 10^{-3} compensated sample compared to that of the 0.9-eV defect peak, and the band-edge peak in undoped samples. The defect peak has approximately the same temperature dependence as the optical band gap.[19] However, the peak in the compensated sample has a substantially larger temperature dependence, which is also a characteristic of the band-edge luminescence peak.[3] Thus again the compensated sample is found to have the character of the band-edge transition.

In Fig. 9 we show the luminescence peak energy for nominally compensated samples as a function of the doping level. The continuous evolution of the peak from the value of ~1.4 eV in undoped material is now clearly evident. Up to doping levels of 10^{-4} the shift is small but at the highest limit investigated (3×10^{-3}) the shift is almost 0.5 eV. This large and continuous change is one of the most striking features of the compensated material. The same tendency is seen in the singly doped material, but the effect is much smaller, as can be seen by comparing Figs. 3 and 9. Figure 10 shows the enhancement of the total luminescence intensity for nominally compensated samples compared to the equivalent doped samples. There is an increase of efficiency at all doping levels with the relative change getting larger as the doping level increases.

Finally in Fig. 11 is shown the luminescence decay of a $10^{-3}[PH_3]$, $1.5 \times 10^{-4}[BH_3]$ compensated sample compared to the decay of the 0.9-eV defect

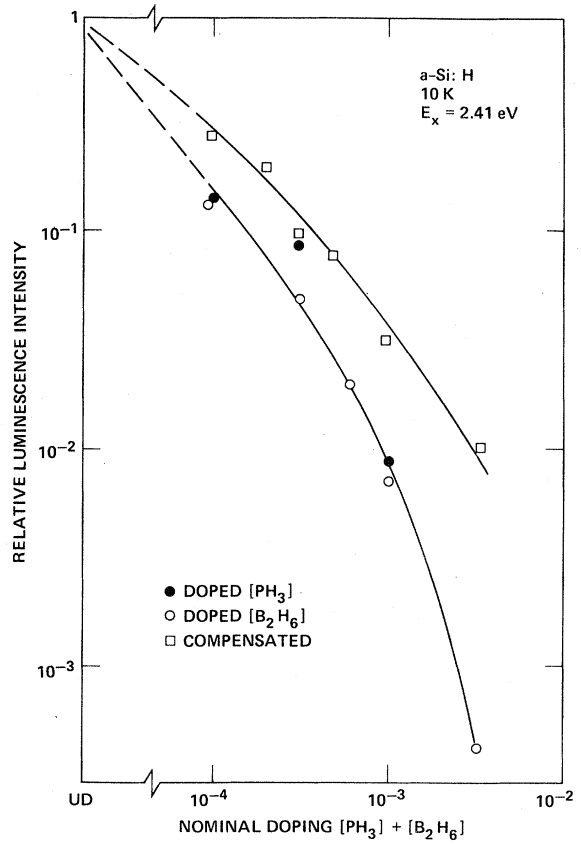

FIG. 10. Comparison of the luminescence intensity of doped samples and nominally compensated material.

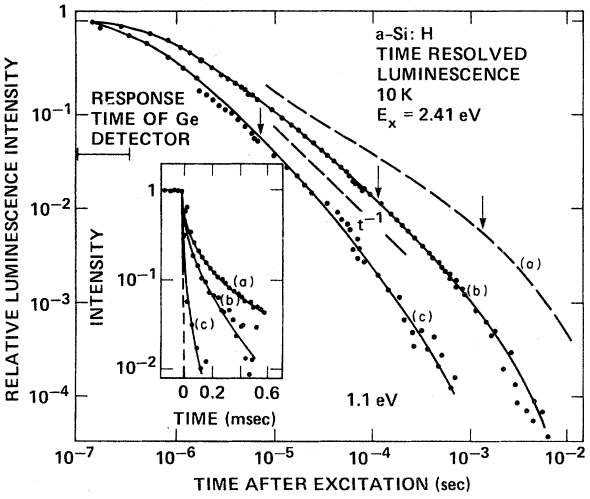

FIG. 11. Luminescence decay of a compensated sample (b) and the 0.9-eV defect peak (c) compared to the decay of undoped samples (a). The arrow indicates where the slope of the decay is −1 and is a rough measure of the average decay time. The insert shows the decay after a long (5-msec) pulse for the same samples.

band in a $10^{-3}[PH_3]$ sample and to an undoped sample. The decay is measured at the peak of the luminescence spectrum using a cooled Ge detector with a minimum time constant of 300 nsec. The arrows in Fig. 11 indicate the time at which the intensity decays as t^{-1} and is a rough measure of the peak in the distribution of decay times.[3] In the compensated sample this time is about an order of magnitude lower than in the undoped sample. However, the decay is broader and the intensity does not drop sharply until ~1 msec, so that the mean lifetime is in fact not much below that of the undoped samples. This result is confirmed by measurements of the decay after a long excitation pulse, also shown in Fig. 11, which is a more direct measurement of the mean decay time. The similar decay times and the broad distribution of the undoped and compensated sample suggests that the same mechanism operates, namely radiative tunnelling, and that the electron states are similar in the two materials. The 0.9-eV defect peak also has a distributed decay, but a substantially smaller mean lifetime. A curious feature of the decay in the compensated sample is that despite the fairly low quantum efficiency (5% of the undoped sample), there is no sign of an initial fast nonradiative process. The most likely explanation seems to be that the nonradiative decay is sufficiently fast that it is not detectable given the time constant of the apparatus. This perhaps indicates a modified nonradiative mechanism compared to that operating in undoped samples, and requires further investigation.

B. Electron spin resonance

1. Singly doped samples

The samples used for the single doping sequence were deposited on 5×10 mm^2 Corning 7059 substrates to a thickness ~7 μm. For reasons described below, no light was allowed to fall on the samples on cooling to, or initially measuring at, 30 K. For the deposition conditions used, no equilibrium ESR signal due to the sample is observed for doping less than $\sim 10^{-3}$. From a massive sample of about 50 mg deposited on aluminum foil we know that the spin density $N_s \leq 3 \times 10^{15}$ cm^{-3} for the undoped sample of this sequence. At doping levels above $\sim 10^{-3}$, equilibrium ESR is observed in both p- and n-type samples, with a spin density which increases rapidly with doping. As shown in Fig. 12(a), boron doping gives a broad line at $g = 2.013$ and phosphorus doping a narrow line near $g = 2.004$, and similar results are reported by others.[7,9] Since at these doping levels the Fermi energy is very near the band edge, the data confirm our previous identification of these ESR lines

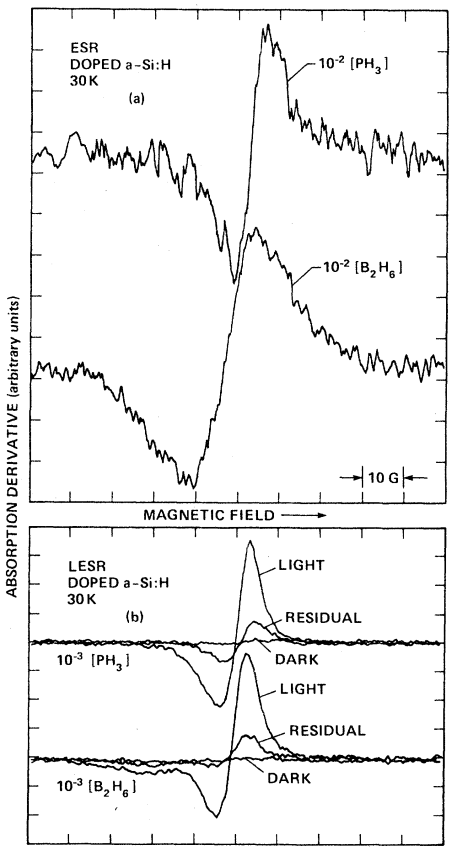

FIG. 12. (a) Equilibrium ESR data for heavily doped *a*-Si:H; (b) ESR spectra showing the absence of an equilibrium (dark) signal, the LESR line and the residual line.

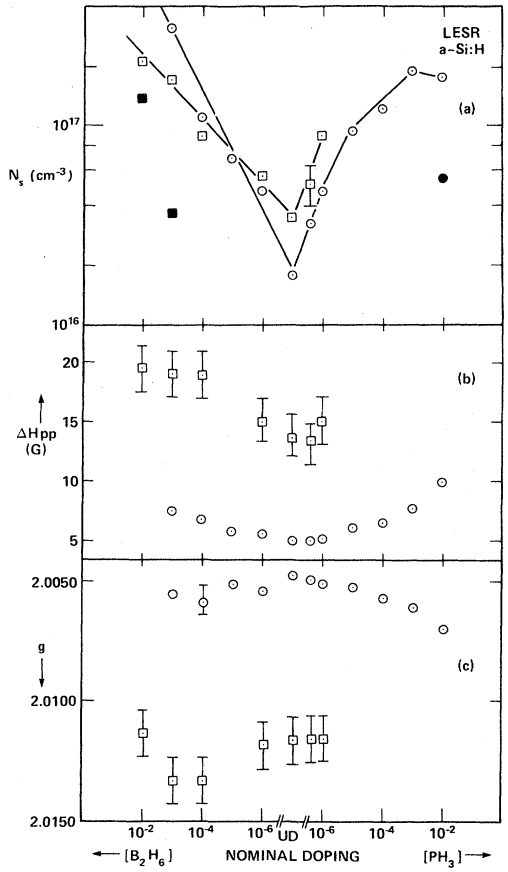

FIG. 13. LESR data for singly doped *a*-Si:H showing (a) the spin densities; (b) the peak-to-peak widths; and (c) the *g* values. The broad line is represented by squares and the narrow lines by circles. The closed data points in (a) are equilibrium ESR data on the only samples with detectable signals.

as band tail holes and electrons. Our identification of these lines is opposite to that previously suggested by Kaplan,[25] based on a comparison of the *g* shifts in amorphous and crystalline Si.

Figure 12(b) shows a sequence of ESR experiments for two representative samples. The "dark" curves are ESR signals before any optical excitation. The "light" curves are obtained during 647.1-nm irradiation. Finally, the "residual" curve is a metastable signal that remains after the illumination is stopped, and is discussed further below. In Fig. 13(a) we show a plot of the LESR spin densities for a constant excitation intensity of ~150 mW/cm^2 at 647.1 nm. The spin densities are obtained from the data by assuming that the spins are distributed uniformly through the samples. The absorption depth at 30 K for 647.1 nm is about 3 μm, and we further neglect the variations which might arise from absorption edge shifts from sample to sample. Under these circumstances the spins are clearly not uniformly distributed. However, the errors involved in these assumptions are reduced by the fact that the intensity dependence of LESR is strongly sublinear.[11] In any case, because the LESR spin densities depend on the lifetimes of the optically excited paramagnetic states, and so measure an undetermined fraction of the states, we can determine here only trends in the density of states associated with the nonequilibrium process. The measurements are carried out at 30 K because, (1) as shown in earlier work, 30 K is low enough that the lifetimes have become approximately temperature independent,[26] whereas (2) 30 K is high enough that the ESR signals are negligibly affected by saturation at the lowest usable microwave powers.[8]

Figure 13(a) indicates that as doping increases, either *p* or *n* type, the narrow and broad spin densities increase over that of the undoped material. In general the *p*-type material contains both broad and narrow lines in roughly equal density, while in *n*-type material the broad line is absent at dop-

ing levels above $10^{-6}[PH_3]$. The g values and widths are shown in Figs. 13(b) and (c) for different doping levels. In undoped samples the narrow line is below $g = 2.005$ with $\Delta H \sim 5$ G and is attributed to conduction band tail electrons.[10] With increased doping both the g value and ΔH get larger. We attribute this result to an increasing dangling-bond contribution at $g \sim 2.0055$. Unfortunately the two lines are never resolved in the ESR spectra, and we believe that this is because their width is larger than their separation (~2 G). The interpretation of the data is further complicated by a continuing shift to larger g value at high doping level. We presume that this shift of the dangling-bond position is due to the high dopant concentration or to the high carrier density. This model of the change in character of the narrow line is supported by the increasing LESR spin density which contrasts with our expectation that the band tail resonance will decrease in density with doping because the luminescence lifetime decreases. Also previous results on $10^{-3}[PH_3]$ and $10^{-3}[B_2H_6]$ demonstrate the dangling-bond character of the narrow line through the temperature dependence of the LESR.[10]

2. *Compensation*

Figure 14 presents the results of LESR in compensated samples, none of which has any detectable equilibrium ESR at 30 K. In this figure, the spin densities are plotted on a linear scale for samples about ~1.2 μm thick. The LESR generally consists of two signals, the dangling-bond line ($g = 2.0055$, $\Delta H_{pp} \sim 7.5$ G) and a broad line at higher g values. An outstanding feature of the LESR variation with doping is the disappearance of the dangling-bond line at the nominal compensation value. Since the defect signal is absent in both LESR and ESR, and E_F is near midgap, we can conclude that the dangling-bond density is greatly reduced. In this sense the compensated material is similar to undoped material. Deviations in doping away from compensation seem to indicate that p-type material has a greater dangling-bond density than n-type which is a similar result as the singly doped samples at the high doping levels [see Fig. 13(a)].

Although the broad line in the compensated material appears to be the same as in undoped and singly doped samples, in fact it has several different properties. Firstly, the spin-density peaks near nominal compensation whereas the results in Fig. 13(a) show the broad line increasing as E_F moves towards the band edge. Secondly, the broad line in singly doped samples is symmetric and stays symmetric in saturation. The broad line in compensated samples on the other hand, is asymmetric with a tail towards high g values. Saturation enhances the asymmetry, with the high g-value components of the line saturating at lower power. A final observation about the broad LESR line is the larger g values (above 2.015) with a distinct shift to lower g values as E_F moves toward the conduction band (for both series of double doping). The maximum observed shift brings the line center

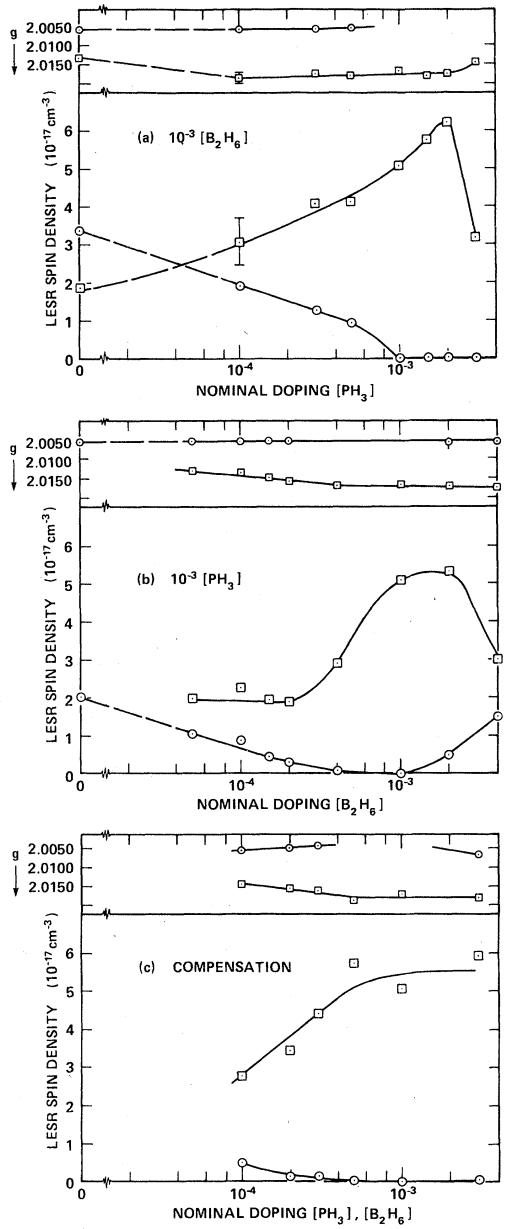

FIG. 14. LESR data in compensated samples. (a) g values and spin densities of $10^{-3}[B_2H_6]$ and variable boron concentrations. (b) g values and spin densities of $10^{-3}[PH_3]$ and variable boron concentrations. (c) g values and spin densities of nominally compensated samples.

to a g value characteristic of the broad line in singly doped samples. From these differences we infer that the states giving the broad line in compensated samples differ from the states in undoped or singly doped material. However, because the changes are slight, we expect that their general description as hole traps is preserved.

In Fig. 14(c) we plot the results of LESR in the series of samples, all nominally compensated, with increasing total level of dopant. For dopant concentrations above 5×10^{-4}, the observations of the preceding section are essentially repeated. The resonance consists of the broad line with g value shifted above 2.015, and the defect line is absent. For dopant concentrations below 3×10^{-4}, the g value and intensity of the broad line decrease rapidly. Simultaneously, the narrow defect line emerges. This behavior qualitatively resembles the rapid shift in luminescence peak energy discussed in Sec. III A.

3. *Residual ESR*

A new and interesting feature of the ESR data is that when the light is turned off, an appreciable signal remains. This residual signal can be seen with remarkably weak illumination because it is generated with approximately unity quantum efficiency initially but quickly saturates at a total number of spins which is proportional to the sample thickness indicating a bulk rather than surface effect. The signal anneals out in a few minutes at ~80 K. Figure 15 shows the residual signals observed in the same set of samples as in Fig. 13. Equivalent residual signals are observed in the compensated samples. The variation of spin density with doping is qualitatively similar to the LESR. Again there is a doping-related increase of the defect signal over the undoped density. The spin densities are about a factor of 5 smaller than and approximately proportional to the LESR signals. We note that both residual hole and electron centers are observed in p-type material, whereas only the hole line is ever observed in the annealed equilibrium signal.

At present we do not have a clear interpretation of the residual signal, and this effect deserves further study. The data demonstrate that carriers can be excited, whose lifetime is indefinitely long at low temperatures. This is a remarkable result in the case of the narrow electronlike resonance in the p-type material, because one would expect that the large density of holes would ensure that the minority carriers would recombine very rapidly. A possible explanation is that carrier diffusion tends to separate the electrons and holes by a reasonably large distance, either because of

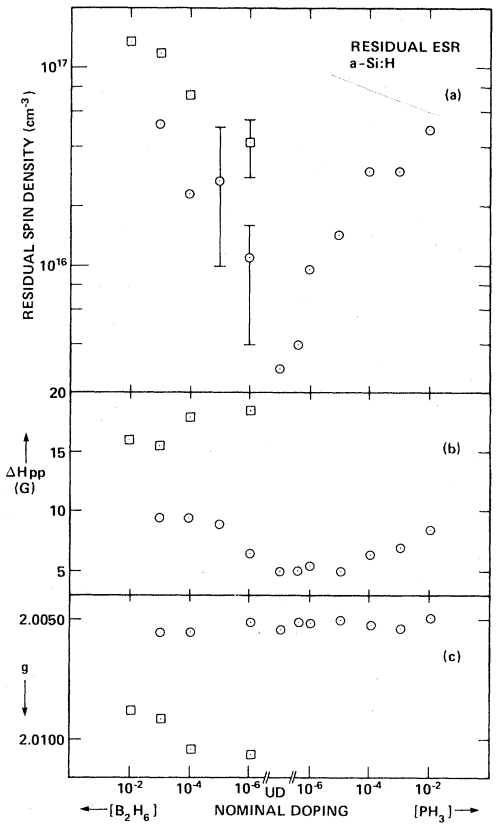

FIG. 15. (a) Spin densities, (b) peak-to-peak linewidths, and (c) g values of the residual ESR signal in singly doped samples.

a surface space charge, or because of their very different mobilities. Microstructural inhomogeneities may also be involved. If the dielectric relaxation time at 30 K is sufficiently long, the nonequilibrium carriers may be metastable because no recombination channels are available.

C. Optical absorption

In view of the large changes in the luminescence peak position, it is of interest to determine the shift of the optical gap in the doped and compensated samples. Figure 16(a) shows examples of part of the absorption edge of a $10^{-3}[PH_3]$ sample and a $10^{-3}[PH_3]$, $4\times10^{-3}[B_2H_6]$ sample. The addition of boron shifts the absorption to low energy and also broadens the edge. The energy E_{04} at which the absorption coefficient is 10^4 cm^{-1} is shown in Fig. 16(b), for the complete compensation series. There is a systematic shift of the band gap by about 0.1 eV. As can be seen by comparing Fig. 16 with Fig. 7 the shift of E_{04} is much smaller than the corresponding shift of the luminescence peak but the boron dependence is of

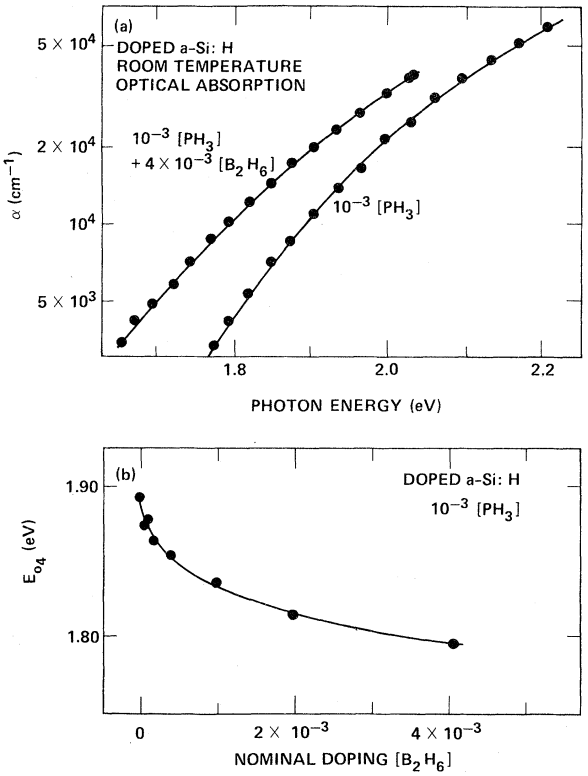

FIG. 16. (a) Portion of the absorption edge of two doped and compensated samples. (b) Value of E_{04} (energy at which $\alpha = 10^4$ cm^{-1}) for a compensation series.

similar form. We find a similar result for the series of nominally compensated samples as shown in Fig. 9. Again the shift of E_{04} is proportional to the shift of the luminescence peak, but the shift of the luminescence is 4–5 times larger.

IV. DISCUSSION

A. Summary

The ESR data indicate that the dangling-bond density increases with doping, but is reduced by compensation, and that compensation introduces new hole states. From the luminescence data we infer that doping introduces nonradiative defects. Compensation apparently reduces the defect density, but the luminescence energy is strongly shifted in energy, which indicates the presence of new localized states. In Sec. IVC we argue that the new states are hole traps. Thus the results of the two experimental probes merge into a single consistent model with the following properties:

(a) Doping introduces nonradiative defects of the dangling-bond type, and compensation reduces their density.

(b) Compensation results in new hole traps above the valence band from which radiative recombination can occur.

The remainder of this section describes the evidence for this model in more detail, and discusses the reason for the change in the localized state distribution and density.

B. Doped samples and mechanisms of defect incorporation

The data presented here coupled with previous results provide very strong evidence that doped samples have a much larger defect density than the corresponding undoped samples. The observation of a large decrease in the luminescence efficiency is in itself a clear indication of an increase of nonradiative states in the gap. The temperature dependence (Fig. 5), intensity dependence (Fig. 4), and decay data provide further evidence of additional states in the gap. In addition the presence of the 0.9 eV defect luminescence, the observation of the $g = 2.0055$ LESR resonance and the correlation of their temperature dependencies,[10] all indicate that the states in the gap are predominantly of the dangling-bond type. Unlike the undoped samples, we do not have an accurate measure of the defect density in the doped samples from the dark ESR. However, we can make an estimate by assuming that the same relation between luminescence efficiency and dangling-bond density holds as in the undoped samples. This assumption remains to be confirmed but a similar procedure has been used by Austin *et al.*[6] Analyzing the data on this basis gives the results shown in Fig. 17. The LESR spin density depends on the light intensity and represents an unknown fraction of the defects. This measurement is therefore only a lower limit, and is also shown in Fig. 17 with consistent results. These data show that doping introduces a very large density of defects, of order 1% of the doping concentration. This conclusion is consistent with the general observation that doped a-Si:H has rather poor electrical properties.

There seem to be two plausible explanations for the increase in dangling-bond density with doping. It is well known that for undoped samples the dangling-bond density is very sensitive to the deposition conditions,[2] and densities ranging over three orders of magnitude can result. Thus it is possible that the presence of the dopant gases PH_3 and B_2H_6 may alter the plasma chemistry in such a way that films with a very large dangling-bond density result. Some evidence for a large effect of the dopants on the plasma properties is the change in deposition rate observed for both dopant gases shown in Fig. 1. Also the results from var-

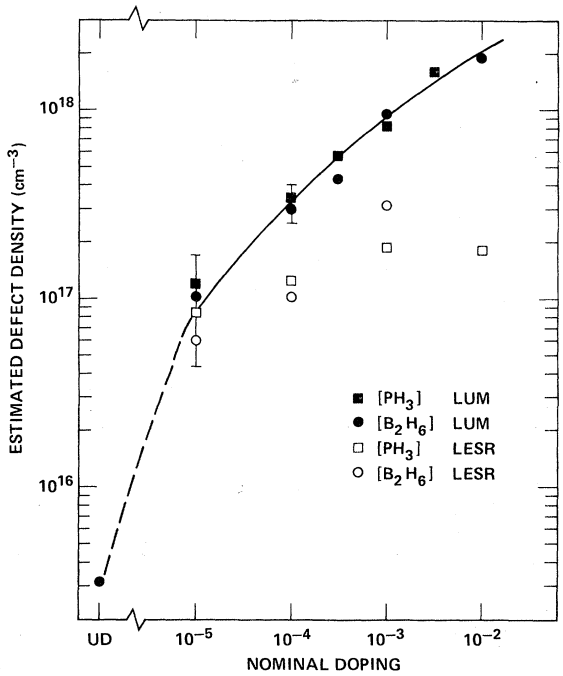

FIG. 17. Estimated defect density obtained from the luminescence and ESR data as described in the text.

ious laboratories differ in the amount of dopant required to quench the luminescence (see Fig. 3). However, the infrared spectra give no evidence of a gross change in the bonding configurations of the compensated material, and columnar growth, usually associated with a high defect density, is not observed.

The alternative explanation of the defects is that they are an inherent consequence of the shift of the Fermi energy. This is the mechanism of autocompensation which is well known to occur in II–VI and III–V crystalline semiconductors. The defects are incorporated because they tend to move the Fermi energy towards midgap thereby reducing the total electronic energy. For example, in the absence of defects, a phosphorus donor has an electron in the donor level, believed to be within the conduction band tail.[14,24] On the other hand, if the donor is compensated by a dangling bond, the extra electron will move to the dangling-bond level which is believed to be 0.2–0.4 eV lower in energy.[19] The energy gained makes the formation of dangling bonds more favorable.

Within the autocompensation model it is possible that the defects are formed in direct association with the dopant as a defect-impurity complex. Such complexes are well known in crystalline semiconductors and are generally believed to be the origin of the autocompensation mechanism.[27] The vacancy-impurity complex is the prime example of such a defect, and its structure in crystalline silicon is shown in Fig. 18(a).[28] It is of interest to the present case because the defect has the following properties:

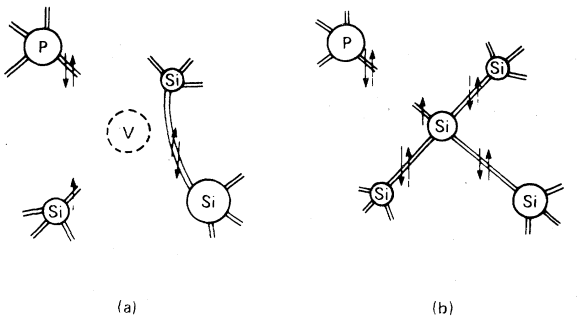

FIG. 18. Possible structures for impurity-defect complexes in doped a-Si:H.

(1) It leaves the impurity in its favored valence configuration (i.e., threefold-coordinated phosphorus). It is generally believed that a large fraction of dopant atoms in a-Si:H will be in this bonding configuration.

(2) It results in a defect with dangling-bond character because the two remaining dangling bonds reconstruct. Thus the defect will have the correct electronic properties.

(3) It maintains the fourfold coordination of the surrounding matrix. The defect therefore has the correct topology for the surrounding lattice.

In an amorphous network the structural constraints on the type of defect are reduced compared to the crystal. A similar defect can be obtained simply by substituting a phosphorus atom for a silicon atom, and disturbing the network slightly, as illustrated in Fig. 18(b). In addition, for defects of the type shown in Fig. 18(a), one might expect hydrogenation, rather than reconstruction of the additional dangling bonds. A wide variety of related structures is clearly possible.

We therefore propose that the most likely mechanism of defect incorporation is a combination of autocompensation and the formation of complexes. We assume that both tend to lower the energy for defect formation E_D which we can write as

$$E_D = E_D^0 - \Delta E_1 - \Delta E_2 ,$$

where E_D^0 is the formation energy in undoped material, ΔE_1 represents the electronic contribution from the difference between the donor level and the defect level, and ΔE_2 represents the lower energy for the formation of a complex. Of course, since the plasma deposition process is not in thermodynamic equilibrium, the defect energy is not the only factor determining the concentration. However, additional defects will certainly be favored if the energy is lowered.

One method of distinguishing between different mechanisms is by compensation. In this way the impurity density can be changed independently of the Fermi energy position. The discussion of the defects will therefore be continued after the compensated material has been discussed.

C. Compensated material

The two important features of the luminescence data of compensated samples are the shift of the peak to low energy and the change of intensity. The shift of the luminescence is much larger than the shift of the optical gap as measured by E_{04}, and so the transition must involve some localized states of larger binding energy than in undoped samples. Despite this the temperature dependence of the luminescence intensity is the same as for an undoped sample of comparable quantum efficiency. Since the thermal quenching is interpreted as the thermally activated diffusion of electrons in the band tails,[3,5] the results indicate that the conduction band tail is not significantly broadened. We also find that the luminescence radiative decay in compensated samples is similar to the undoped samples. This result again suggests little change in the conduction band tail, because the decay times are believed to be determined by the electron wave function.[3] Drift mobility measurements also find that the donor levels are located within the conduction band tails which is itself not greatly modified by doping.[24] If the conduction band tail is unchanged then we must conclude that the shift of the luminescence is due to the presence of additional states above the valence band. We suppose that a broad band of states are introduced as a result of compensation. As the density of these states increases, holes will be able to thermalize further into the gap, explaining the progressive shift to low energy of the luminescence peak. The model is shown schematically in Fig. 19. The extra states will give an extrinsic absorption band which readily accounts for the broadening and shift of the absorption edge.

The experimental results show that there is a similar, but smaller shift to low energy of the luminescence in singly doped material at doping levels above 10^{-3} (see Fig. 3). It is also known that there is a broad extrinsic tail to the absorption edge, particularly in the boron doped material.[21,29] Photoemission also gives direct evidence of states above the valence band in material doped by PH_3.[30] It seems therefore that states above the valence band may be a general consequence of heavy doping. However, it is clear that in the compensated samples the effect of the two dopants are not simply additive, but there is some cooperative process that leads to the much larger shift of the luminescence. We have already shown from the SIMS measurements of concentrations in Table I, that there is a cooperative mechanism that tends to equalize the boron and phosphorus concentrations. We therefore suggest that the states above the valence band in the compensated material arise from boron-phosphorus pairs, or some other complex involving both impurities. Donor-acceptor nearest-neighbor pairs are strongly favored by the Coulomb interaction and are common in semiconductors (e.g., CdO in GaP).[31] Such a complex in a-Si:H might reasonably be expected to act as a hole trap. However, in the absence of any micro-

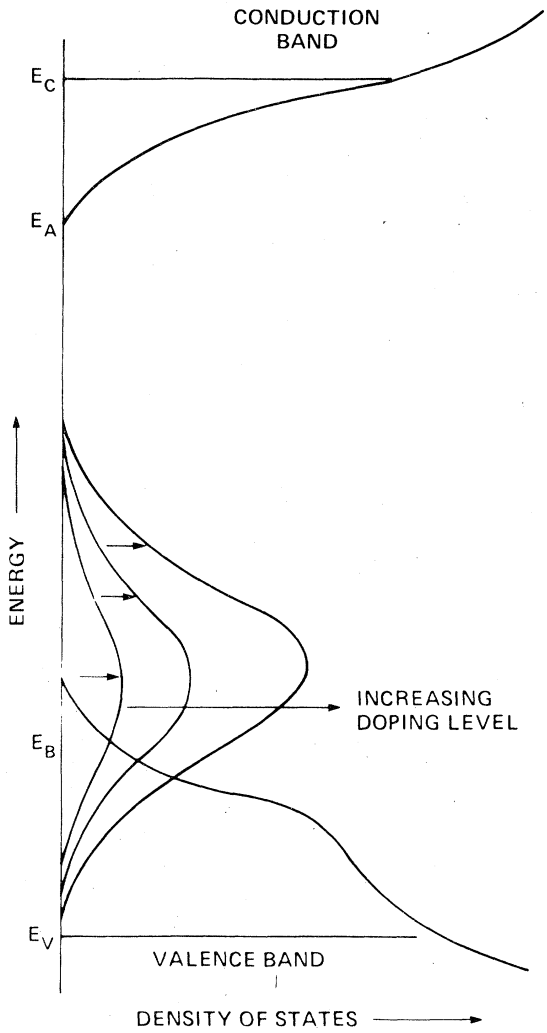

FIG. 19. Schematic density-of-states diagram showing the suggested states above the valence band introduced by compensation. The arrows are intended to illustrate the mean energy to which holes thermalize. The shift of this energy would explain the change in the luminescence peak energy.

scopic structural data to identify the center, we have no further confirmation of this model. We also note that Reimer *et al.*[32] have deduced from proton NMR that boron clustering occurs in B-doped *a*-Si:H. This is another indication that dopant incorporation is a complex process.

These states above the valence band replace the band tail as the hole states participating in the radiative transition and therefore explain the shift of the peak. The states are therefore not expected to also determine the nonradiative processes for which some other states, such as dangling bonds, are presumably responsible. One of our major results is that compensation increases the luminescence efficiency. The increase is by a factor of 10 and 3.5 for the series shown in Figs. 7 and 8, respectively. Based on the model that the nonradiative recombination occurs through states in the gap, we conclude that compensation decreases the density of these states. However, compensation is not fully effective in restoring the luminescence intensity and this indicates that even in the compensated samples some nonradiative centers remain.

In the compensation series the maximum luminescence intensity occurs at the nominal compensation level in the data of Fig. 8 (variable PH_3), but on the *n*-type side for the series shown in Fig. 7 (variable B_2H_6). These results can be understood qualitatively on the basis of two counteracting mechanisms. These are that compensation tends to decrease the defect density, whilst the additional doping tends to increase it. We believe that boron is more effective at introducing defects than phosphorus at these high doping levels, and the evidence is that above 10^{-3} doping the luminescence decreases faster in boron doped material. Thus in the series with variable B_2H_6 the maximum luminescence intensity is shifted towards lower levels of boron.

The LESR data provides some specific information about the localized states in the samples and strongly supports the above model. We find that the dangling-bond density decreases upon compensation and is in fact undetectable at nominal compensation. In the compensated series the LESR is dominated by the broad resonance near $g = 2.015$ which we have attributed to hole states of different origin from those observed in undoped samples. The model proposed above is that compensation introduces additional hole states above the valence band to which holes thermalize rapidly. We therefore associate the broad resonance with these radiative states since the maximum observed LESR spin density occurs near the compensation point where the maximum luminescence intensity also occurs. As described above, these states are believed to have a different microscopic origin than the hole states in undoped material and we suggest that the small change in ESR line shape is an indication of the different character.

D. Origin of the defect states

We now return to the question of the mechanism by which defects are incorporated in doped material. The compensated samples demonstrate that the dangling-bond density decreases as the Fermi energy is moved towards midgap. This result rules out any model that relates the defect density solely to the presence of dopants. Instead we believe that the changes with doping and compensation provide good evidence for the autocompensation mechanism suggested in Sec. IV B. However, the properties of the material are complicated by the observation of extra localized states, believed to be hole traps, introduced by the presence of both dopants. Those states are in addition to any impurity-defect complexes, etc., that might occur in singly doped samples.

It is clear that as more components are added to the material, the number of possible defects greatly increases. Much more work needs to be done to confirm the identity of the dominant defect states. For technological uses it is obviously desirable to find some way of reducing the density of states in the gap in doped *a*-Si:H. Since our results suggest that the defect states are largely an intrinsic result of doping through the autocompensation mechanism, it may prove difficult to reduce their density.

V. CONCLUSIONS

Measurements are reported of the luminescence, ESR, optical absorption, conductivity, and composition of *a*-Si:H doped and compensated with phosphorus and boron. From the data various properties are inferred.

(1) Doping with either phosphorus or boron introduces dangling-bond-type defects into the material. The density of defects is of order 1% of the dopant concentration, but this value may be sensitive to the deposition conditions.

(2) Various mechanisms for the introduction of defects are discussed. The evidence of the compensated samples indicates that autocompensation is an important mechanism. We suggest that the dangling-bond defects are likely to enter the structure as defect-impurity complexes, and some possible configurations are suggested.

(3) Compensation reduced the dangling-bond density. The reduction is seen directly by ESR and by inference from the increase in luminescence efficiency. Compensation also introduces new states

above the valence-band edge. We suggest that the microscopic origin of these states is a boron-phosphorus complex.

(4) A metastable, residual ESR signal is discovered in doped and compensated a-Si:H after illumination at low temperatures. Charge separation by diffusion is a possible explanation.

(5) The broadening of the optical-absorption edge is attributed to extrinsic absorption from the hole states introduced by compensation.

(6) The composition of compensated samples for specific dopant gas concentrations is not simply related to the equivalent singly doped material. Instead there is a cooperative interaction which tends to equalize the dopant concentrations.

(7) The dopants change the deposition rate by an amount which greatly exceeds their relative concentration in the films. These last two results illustrate the complexities of the plasma chemistry during deposition.

Note added in proof. Recent measurements of the extrinsic absorption tail in these samples by Jackson and Amer (unpublished) agree with the defect densities obtained from the luminescence data as shown in Fig. 17.

ACKNOWLEDGMENTS

The expert technical assistance of R. Lujan is gratefully acknowledged. This work was partially supported by the Solar Energy Research Institute under Contract No. XJ-0-9079-1.

[1]R. Fischer, *Topics in Applied Physics*, edited by M. H. Brodsky (Springer, Berlin, 1979), Vol. 36.
[2]R. A. Street, J. C. Knights, and D. K. Biegelsen, Phys. Rev. B 18, 1880 (1978).
[3]C. Tsang and R. A. Street, Phys. Rev. B 19, 3027 (1979).
[4]R. A. Street, Philos. Mag. B 37, 35 (1978).
[5]J. Noolandi, K. M. Hong, and R. A. Street, Solid State Commun. 34, 45 (1980).
[6]R. A. Street, Phys. Rev. B 23, 2967 (1981).
[7]J. Stuke, *Proceedings of the Seventh International Conference on Amorphous and Liquid Semiconductors*, edited by W. E. Spear (University of Edinburgh, Edinburgh, 1977), p. 406.
[8]D. K. Biegelsen, Solar Cells 2, 421 (1980).
[9]S. Hasegawa, T. Kasajima, and T. Shimizu, Philos. Mag. 43, 149 (1981); J. Stuke (unpublished).
[10]R. A. Street and D. K. Biegelsen, Solid State Commun. 33, 1159 (1980).
[11]J. C. Knights, D. K. Biegelsen, and I. Solomon, Solid State Commun. 22, 133 (1977).
[12]W. E. Spear and P. G. Le Comber, Solid State Commun. 17, 1193 (1975).
[13]P. G. Le Comber and W. E. Spear, in *Structure and Excitation of Amorphous Solids-Williamsburg, Virginia, 1976*, Proceedings of an International Conference on Structure and Excitation of Amorphous Solids, edited by G. Lucovsky and F. L. Galeener (AIP, New York, 1976), p. 285.
[14]A. Madan, P. G. Le Comber, and W. E. Spear, J. Non-Cryst. Solids 20, 239 (1976).
[15]J. C. Knights, T. M. Hayes, and J. C. Mikkelsen, Phys. Rev. Lett. 39, 712 (1977).
[16]R. Fischer, W. Rehm, J. Stuke, and U. Voget-Grote, J. Non-Cryst. Solids 35 & 36, 687 (1980).
[17]I. G. Austin, T. S. Nashashibi, T. M. Searle, P. G. Le Comber, and W. E. Spear, J. Non-Cryst. Solids 32, 373 (1979).
[18]C. Tsang and R. A. Street, Phil. Mag. B37, 601 (1978).
[19]R. A. Street, Phys. Rev. B 21, 5775 (1980).
[20]J. C. Zesch, R. A. Lujan, and V. R. Deline, J. Non-Cryst. Solids 35 and 36, 273 (1980).
[21]J. C. Knights, in *Structure and Excitation of Amorphous Solids-Williamsburg, Virginia, 1976*, Proceedings of an International Conference on Structure and Excitation of Amorphous Solids, edited by G. Lucovsky and F. L. Galeener (AIP, New York, 1976), p. 296.
[22]G. Lucovsky, R. J. Nemanich, and J. C. Knights, Phys. Rev. B 19, 2064 (1979).
[23]J. C. Knights and R. A. Lujan, Appl. Phys. Lett. 35, 244 (1979).
[24]D. Allen, P.G. Le Comber, and W. E. Spear, *Proceedings of the Seventh International Conference on Amorphous and Liquid Semiconductors*, edited by W. E. Spear (University of Edinburgh, Edinburgh, 1977), p. 323.
[25]D. Kaplan, *Fourteenth International Conference on the Physics of Semiconductors*, edited by B. L. H. Wilson (Institute of Physics, London, 1978), p. 1129.
[26]D. K. Biegelsen and J. C. Knights, *Proceedings of the Seventh International Conference on Amorphous and Liquid Semiconductors*, edited by W. E. Spear (University of Edinburgh, Edinburgh, 1977), p. 429.
[27]Eg. E. W. Williams and H. B. Bebb, *Semiconductors and Semimetals*, edited by A. C. Beer and R. K. Willardson (Academic, New York, 1972), Vol. 8, p. 321.
[28]G. D. Watkins and J. W. Corbett, Phys. Rev. 134, A1359 (1964).
[29]E. C. Freeman and W. Paul, Phys. Rev. B 20, 716 (1979).
[30]B. von Roedern and G. Moddel, Solid State Commun. 35, 467 (1980).
[31]C. H. Henry, P. J. Dean, and J. D. Cuthbert, Phys. Rev. 166, 754 (1968).
[32]J. A. Reimer, R. W. Vaughan, and J. C. Knights (unpublished).